

# Fabrication of Photovoltaic Cell From Ruthenium Containing Polymer Using Layer By Layer Polyelectrolytes Adsorption Technique

Ka Yan Kitty Man<sup>1</sup>, Kai Wing Cheng<sup>1</sup>, Hei Ling Wong<sup>1</sup>, Chung Yin Kwong<sup>2</sup>, Wai Kin Chan<sup>1\*</sup>, Aleksandra B. Djurišić<sup>2,3</sup>

<sup>[1]</sup>Department of Chemistry, the University of Hong Kong, Pokfulam Road, Hong Kong

<sup>[2]</sup>Department of Electrical and Electronic Engineering, the University of Hong Kong, Pokfulam Road, Hong Kong

<sup>[3]</sup>Department of Physics, the University of Hong Kong, Pokfulam Road, Hong Kong

## ABSTRACT

Multilayer photovoltaic devices were fabricated by the sequence adsorption of different polyelectrolytes. A ruthenium terpyridine complex containing poly(*p*-phenylenevinylene) was used as the polycation layer. This polymer has been shown to exhibit large photo-sensitivity due to the presence of the ruthenium complex, which has relatively long-lived excited state. This polymer absorbs strongly in the visible region at ca. 480-550 nm and it can act as the electron transporter. Sulfonated polyaniline was used as the hole-transporting polyanion layer. The ITO/(polyanion/polycation)<sub>n</sub>/Al devices were found to exhibit photovoltaic properties under the illumination of AM1 solar radiation. The short-circuit current  $I_{sc}$ , open-circuit voltage  $V_{oc}$ , and the fill factor  $FF$  were measured to be 14  $\mu\text{A}/\text{cm}^2$ , 0.84 V and 0.16 respectively. It was found that the power conversion efficiencies of the devices were dependent on the device thickness. This simple layer-by-layer self-assembly method allowed us to control the devices thickness accurately.

Keywords: Electrostatic self-assembly, electrolytes, ruthenium containing polymer, photovoltaic

## 1. INTRODUCTION

Conjugated polymer-based electronic devices are under intensive investigation as they show promising potential application including electroluminescence light emitting diodes (LEDs)<sup>1</sup>, transistors<sup>2</sup> and photovoltaic devices<sup>3</sup>. Many different type of materials like fullerene or polymers with low bandgap have been used in solar cells in order to enhance the power conversion efficiency. Solution spin coating is one of the easiest methods for preparing polymer film. However, the film thickness and surface morphology are difficult to control. For an efficient photovoltaic device, a good mixing of donor and acceptor at the interfacial area is needed for efficient charge generation. Since the excitation diffusion length in conjugated polymer is limited to few nanometers, this electron transfer process is greatly enhanced by a good donor-acceptor interface<sup>4</sup>, which, common spin coating method may not be possible to provide.

A layer-by-layer electrostatic self-assembly (ESA) technique was first developed by Decher and coworkers<sup>5-9</sup>. Their work started from opposite charges of bipolar amphiphiles containing rigid biphenyl cores<sup>10</sup> to polyelectrolytes. The crucial factor for the successful deposition is the surface charges reversal upon adsorption. Polyelectrolytes concentration, ionic strength, pH, dipping time or the nature of solvents can affect the film thickness significantly<sup>11</sup>. Still, this technique provides an easy way to prepare smooth, thin films with thickness precision in the range of a few Angstroms. There seems to have no limitation on the maximum build-up layers. The charged polymer layers are interpenetrated in the order of the layer thickness<sup>12</sup> and the term 'opposite charged layer pair' can be referred as

'bilayer'. By using the ESA technique, devices with bicontinuous interpenetrating active layers and large interfacial area can be constructed. These heterojunction devices allow efficient transport of the photogenerated electrons and holes to the opposite electrodes, leading to devices with improved energy conversion efficiency.

## 2. RESULTS AND DISCUSSION

### 2.1 Synthesis

The ruthenium containing poly(*p*-phenylenevinylene) (Ru-PPV) polycation was synthesized by palladium catalysed Heck coupling reaction. The sulfonated polyaniline (SPAN) polyanion was prepared by the sulfonation of polyaniline (PAn)<sup>13</sup>. Both polymers contained charges on the main chain. The Ru-PPV and SPAN were soluble in *N,N*-dimethylformamide (DMF) and water respectively. Figure 1 shows the synthesis of the polymers.

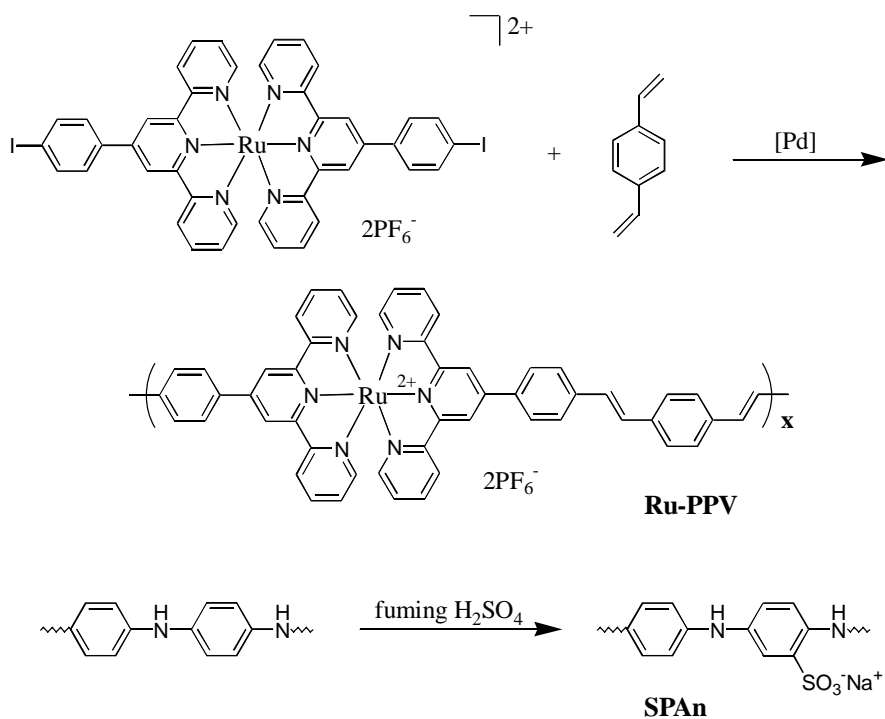


Figure 1. Synthesis of ruthenium functionalised PPV as **polycation** and sulfonated polyaniline as **polyanion**.

## 2.2 Fabrication Of Device – Electrostatic Self-Assembly

In order to provide a charged surface on the substrate for polyelectrolytes to deposit, the indium tin oxide (ITO) glass substrate must be treated prior to use. The clean ITO glass substrates were immersed in 5 wt % (3-aminopropyl)trimethoxysilane in toluene for 16 h to introduce positive charges onto the substrate surface. The substrates were dipped into the polyanion (SPAN with concentration of 0.07 mg/mL dissolved in water) for 15 min, rinse with water and immersed in polycation (Ru-PPV with concentration of 0.09 mg/mL dissolved in DMF) for another 15 min, rinsed with DMF to complete one fabrication cycle. In each cycle, a bilayers of SPAN:Ru-PPV was deposited on the substrate. The Ru-PPV in the device served as the electron-transporting species while SPAN was used as the hole-transporting species.

## 2.3 Optical Properties

According to Figure 2, the electronic absorption spectra of Ru-PPV mainly consist of two parts. The absorption peaks at ca. 380 and 506nm are due to the  $\pi$ - $\pi^*$  transition of the terpyridine ligand and the metal-to-ligand charge transfer (MLCT) transition of the complex, respectively. For SPAN, the  $\lambda_{\max}$  was at 325 nm. All the thin films showed absorption peaks at 325 and 506 nm, which were assigned as the SPAN and Ru-PPV absorption respectively. The absorption intensity increased according to the number of bilayers deposited on the substrates and this proved that the film thickness increased with the number of layers deposited.

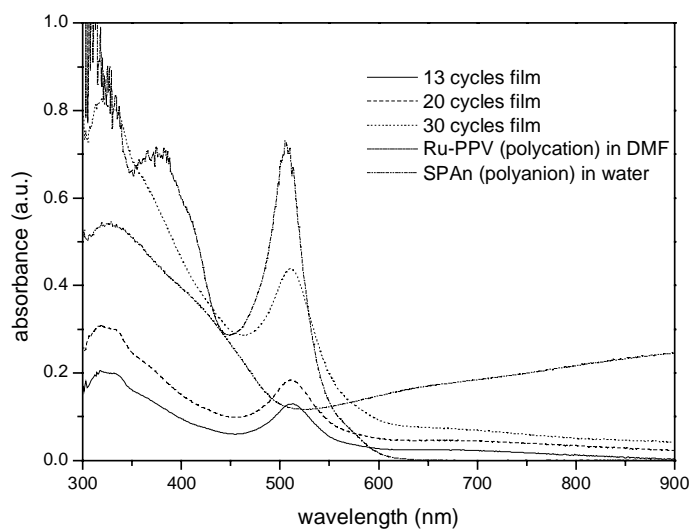


Figure 2. Electronic absorption spectra of polycation, polyanion and films dipped with different number of cycles.

## 2.4 Photovoltaic Properties

In order to test the applicability of the multilayer device for light energy conversion, the devices with various numbers of bilayers were deposited with 40 nm Al as electrode and studied under atmosphere. Figure 3 shows the linear and semi-logarithmic plot of the  $I/V$  curves of a 30 cycles multilayer device in dark and under white-light illumination of a xenon lamp at  $\sim 63 \text{ mW/cm}^2$ .

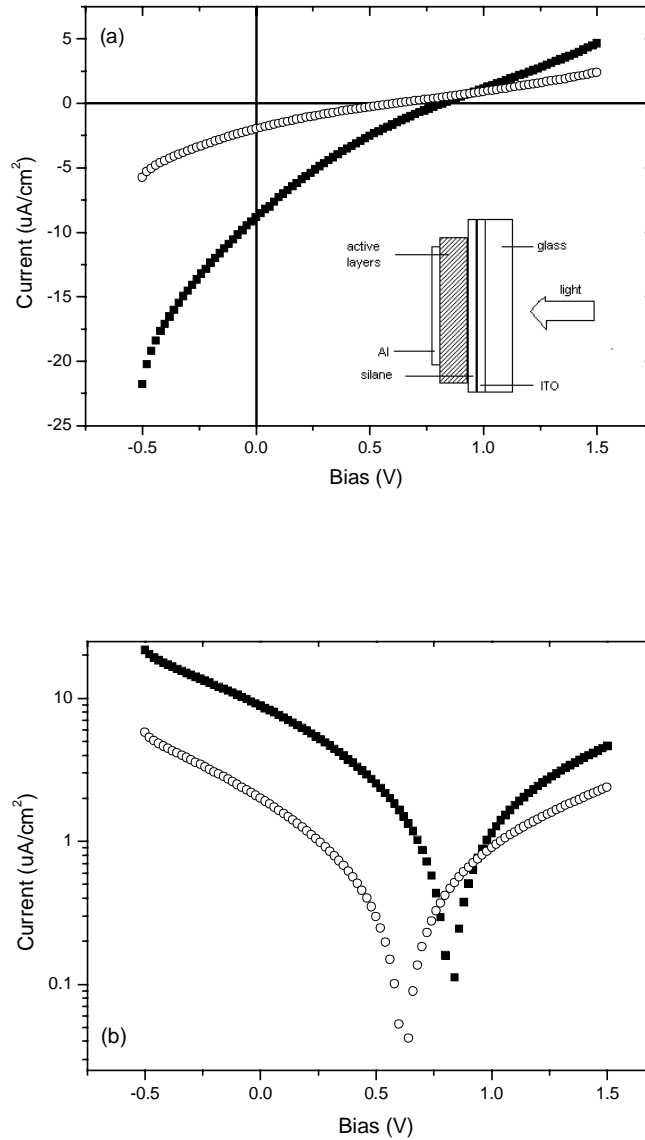


Figure 3. a) Linear and b) semi-logarithmic plot of the current-voltage characteristic for the ITO/silane/polyanion:polycation/Al device in the dark (o) and under  $\sim 63 \text{ mW/cm}^2$  white-light illumination ( $\blacksquare$ ). The insert shows the configuration of the cell.

An open-circuit voltage ( $V_{oc}$ ) of 0.84 V and short-circuit current ( $I_{sc}$ ) of 8.8  $\mu\text{A}/\text{cm}^2$  were obtained. The fill factor ( $FF$ ) was determined to be 0.19 where it is defined as  $(I_{max} \times V_{max}) / (I_{sc} \times V_{oc})$ , with  $I_{max}$  and  $V_{max}$  corresponding to the point of maximum power output. The relatively low  $FF$  may be due to the large serial resistance caused by the defects in the films<sup>14</sup>. All these parameters can inhibit the transfer of holes and electrons generated by photons, causing recombination of charge carriers and results in quenching the energy conversion. The dark current in Figure 3 did not pass through the origin of the graph. One possible reason is the trapping of charges near the polymer interfaces. For the power conversion efficiency ( $\eta_{PCE} = (P_{out}/P_{in}) \times 100 = (FF \times V_{oc} \times I_{sc}/P_{in}) \times 100$ ), it was calculated to be  $2 \times 10^{-2}$  %. Table 1 shows the photovoltaic properties of devices with different number of dipping cycles.

No. of bilayers	$I_{sc}$ ( $\mu\text{A}/\text{cm}^2$ )	$V_{oc}$ (V)	$FF$	$\eta_p$ (%)
13	14.9	0.84	0.16	0.0019
20	12.6	0.68	0.18	0.0017
30	8.8	0.84	0.19	0.0022

Table 1. Photovoltaic properties of films with various numbers of bilayers under  $\sim 63 \text{ mW}/\text{cm}^2$  white-light illumination.

According to Table 1, devices with more number of bilayers have relatively higher power conversion efficiency, probably due to their higher absorption coefficients. From these results, it can be confirmed that the charge dissociation happened at the p-n junction of the polyelectrolytes layer but not the electrode/polymer interface. If the charge dissociation happened at the interface, the thin thickness would not affect the efficiency.

To further study the device performance, the  $I_{sc}$ ,  $V_{oc}$ , and  $FF$  of the 30 bilayers device were compared as a function of white light intensity. From Figure 4, the short circuit current is linearly dependent on the light intensity (increased from 3.6  $\mu\text{A}/\text{cm}^2$  at 24  $\text{mW}/\text{cm}^2$  to 26  $\mu\text{A}/\text{cm}^2$  at 400  $\text{mW}/\text{cm}^2$ ). The open circuit voltage changed from 0.8 V to 0.92 V and  $FF$  decreased from 0.2 to 0.17. Hence the power conversion efficiency at lowest light intensity is about double than that at the highest light intensity.

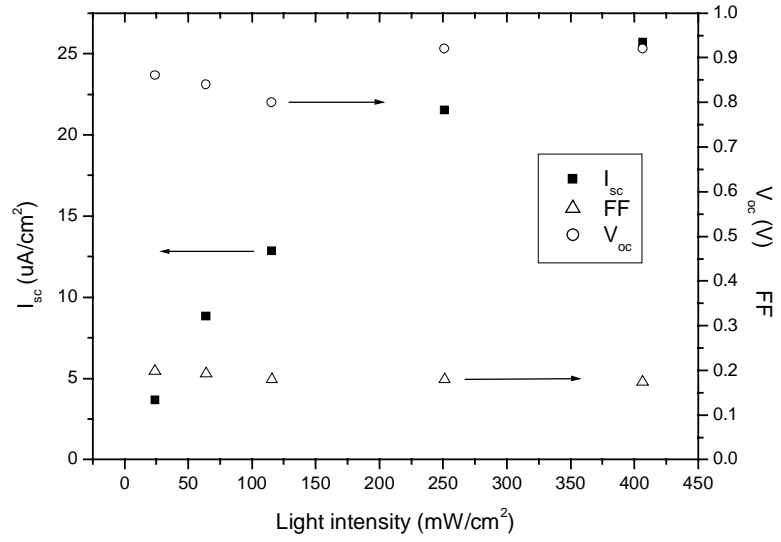
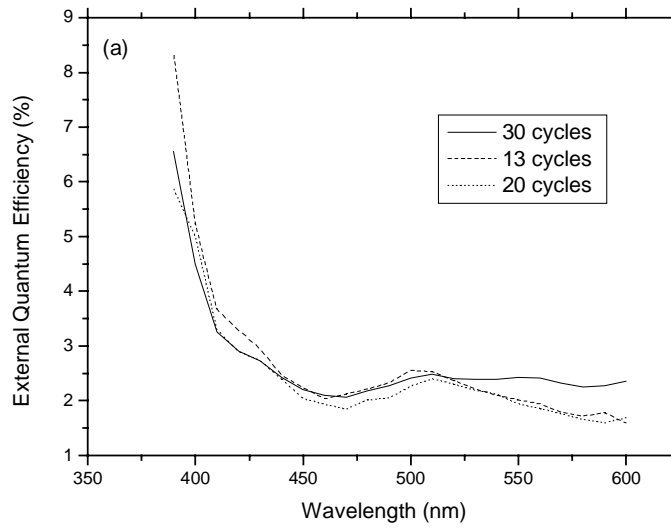


Figure 4. Plot of short circuit current ( $I_{sc}$ ), open circuit voltage ( $V_{oc}$ ), and fill factor ( $FF$ ) as the function of the intensity of the white light.



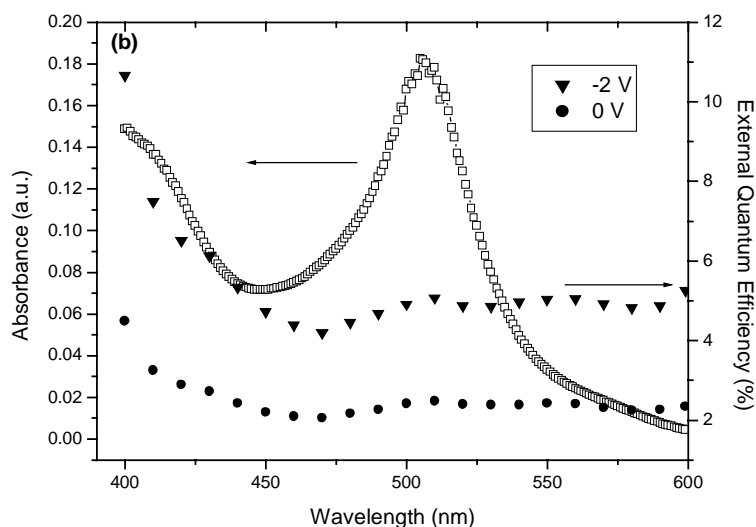


Figure 5. External quantum efficiencies for a) devices dipped with 13, 20 and 30 cycles in 0 V bias and b) device dipped with 30 cycles under a bias of 0 V and  $-2$  V and the corresponding UV-vis absorption.

Figure 5 shows the plot of EQE as the function of the wavelength of incident light. The EQE were independent to the number to cycles dipped in the devices and it closely follows the absorption spectrum of the multilayers thin film. At the maximum of the MLCT absorption band (ca. 500nm) the EQE at 0 V and  $-2$  V bias were about ca. 2 % and 5 % respectively. These devices exhibited low power conversion and external quantum efficiencies because the films were very thin compare to other organic solar cells. As a result, fewer excitations were generated because of the low absorbance. This can be improved by constructing thicker devices. Nevertheless, this self-assembly method provides a new approach in fabricating photovoltaic cells and there are rooms for further improvement.

### 3. CONCLUSION

A series of photovoltaic devices with different number of SPAn:Ru-PPV bilayers was prepared by the layer by layer polyelectrolytes adsorption technique. The devices were characterized and their photosensitising properties were studied. In a 30 cycles multilayer device worked under white-light illumination of a xenon lamp at  $\sim 63$  mW/cm<sup>2</sup>, open-circuit voltage ( $V_{oc}$ ) = 0.84 V and short-circuit current ( $I_{sc}$ ) = 8.8 uA/cm<sup>2</sup> were obtained. The fill factor ( $FF$ ) was calculated to be 0.19. The EQE at 500 nm with 0 V and  $-2$  V bias were about ca. 2 % and 5 % respectively. Photovoltaic devices can be fabricated by using different kinds of n- and p- type polyelectrolytes in order to enhance the exciton generation and the charge transporting processes. It is also possible to fabricate photovoltaic cells with interesting device structures. For example, a mixed layer of photosensitizers that cover the whole visible/NIR region can be used.

#### 4. ACKNOWLEDGMENTS

This work was supported by the Research Grants Council of The Hong Kong Special Administrative Region, China (Project No. HKU 7096/00P) and The Committee on Research and Conference Grants, University of Hong Kong.

#### 5. REFERNECES

1. (a) J.H. Burroughes, *Nature*, **347**, 539, 1990. (b) M. Wohlgenannt, K. Tando, S. Mazumdar, S. Ramasesha, Z.V. Vardeny, *Nature*, **409**, 494, 2001
2. J.H. Burroughes, C.A. Jones, R.H. Friend, *Nature*, **335**, 137, 1988
3. (a) G. Yu, J. Gao, J.C. Hummelen, F. Wudl, A.J. Heeger, *Science*, **270**, 1789, 1995. (b) A. Shah, P. Torres, R. Tscharnner, N. Wyrsh, H. Keppner, *Science*, **285**, 692, 1999
4. A. Dhanabalan, J.K.L. van Duren, P.A. van Hal, J.L.J. van Dongen, R.A.J. Janssen, *Advanced Functional Materials*, **11**, 255, 2001
5. G. Decher, J.D. Hong, J. Schmitt, *Thin Solid Films*, **210/211**, 831, 1992
6. Y. Lvov, G. Decher, H. Möhwald, *Langmuir*, **9**, 481, 1993
7. Y. Lvov, G. Decher, G. Sukhorukov, , *Macromolecules*, **26**, 5396, 1993
8. Y. Lvov, F. Essler, G. Decher, *J. Phys. Chem.*, **97**, 13773, 1993
9. Y. Lvov, H. Haas, G. Decher, H. Möhwald, A. Kalachev, *J. Phys. Chem.*, **97**, 12835, 1993
10. G. Decher, J.D. Hong, *Makromol Chem Macromol Symp*, **46**, 321, 1991
11. P. Bertrand, A. Jonas, A. Laschewsky, R. Legras, *Macronol. Rapid. Commun*, **21**, 319, 2000
12. J. Schmitt, T. Grünewald, G. Decher, P.S. Pershan, K. Kjaer, M. Lösche, *Macromolecules*, **26**, 7058, 1993
13. J. Yue, Z.H. Wang, K.R. Cromack, A.J. Epstein, A.G. MacDiarmid, *J. Am. Chem Soc.*, **113**, 2665, 1991
14. M. Lösche, J. Schmitt, G. Decher, W.G. Bouwman, K. Kjaer, *Macromolecules*, **31**, 8893, 1998